# Complexation of $Cu^{2+}$ by HETPP and the Pentapeptide Asp-Asp-Asn-Lys-Ile: A Structural Model of the Active Site of Thiamin-Dependent Enzymes in Solution

**Gerasimos Malandrinos,[†] Maria Louloudi,*[,†] Yiannis Deligiannakis,[‡] and Nick Hadjiliadis*[,†]**

Laboratory of Inorganic and General Chemistry, Department of Chemistry, University of Ioannina, 45110 Ioannina, Greece, and Laboratory of Physical Chemistry, Department of Environmental and Natural Resources Management, University of Ioannina, Pyllinis 9, 30100 Agrinio, Greece

*Received December 28, 2000*

To obtain structural information on the active site of thiamin-dependent enzymes in solution, we have studied the interactions of $Cu^{2+}$ ions with 2-(α-hydroxyethyl)thiamin pyrophosphate (HETPP), the pentapeptide Asp-Asp-Asn-Lys-Ile surrounding the thiamin pyrophosphate moiety in the transketolase enzyme, and the tertiary $Cu^{2+}$−pentapeptide−HETPP system in aqueous solutions at various pH values. In the binary $Cu^{2+}$−pentapeptide system around physiological pH, the bonding sites were the terminal $NH_2$ group, the aspartate *β*-carboxylates, and a deprotonated peptide nitrogen, while, in the $Cu^{2+}$−HETPP system at the same pH, the Cu(II) was coordinated to the pyrophosphate group and to the pyrimidine N(1′) atom. It is found that, in the tertiary system at physiological pH, the peptide bone offers three coordination sites to the metal ion, and the coordination sphere is completed by two additional phosphate oxygens and the nitrogen N(1′) of the thiamin coenzyme. The stability constants in the tertiary system are higher than those in the simpler $Cu^{2+}$−HETPP and $Cu^{2+}$−peptide systems. The present data show that the coenzyme adopts the so-called S conformation in solution. The importance of our findings concerning the N(1′) coordination and the S conformation in the tertiary system is discussed in conjunction with the role of HETPP as an intermediate of thiamin catalysis.

## Introduction

Thiamin enzymes catalyze the decarboxylation of α-keto-acids and the transfer of aldehyde or acyl groups in vivo.[1] The holoenzymes depend on the cofactors thiamin pyrophosphate (TPP) and $Mg^{2+}$ or $Ca^{2+}$. The cofactor TPP plays a key role in the enzymic mechanism which proceeds through the "active acetaldehyde" intermediates (Scheme 1). These intermediates are formed after nucleophilic addition of a substrate on the C(2) atom of thiamin and subsequent decarboxylation,[1] and they specify the role of the thiazole moiety. Although the importance of the pyrimidine ring has always been recognized, its participation in the catalytic process has never been understood in detail.

In terms of the relative orientation of the thiazolium and pyrimidine ring, the TPP molecule can adopt three different conformations, F, S, and V.[2] In all of the crystal structures of TPP-dependent enzymes, TPP adopts the V conformation, which brings 4′-$NH_2$ close to C(2).[3] On the other hand, it should be noted that, without exception, all of the C(2)-substituted thiamin intermediates which have been either isolated from enzymic systems or synthesized in vitro adopt the S conformation.[4]

In the analyzed crystal structures of thiamin enzymes, the pyrimidine ring is buried in a hydrophobic pocket which is not accessible to solvent, while the diphosphate moiety is embedded in an elaborate network of salt bridges and hydrogen bonds, formed between protein residues, water molecules, and the metal ion.[3] The metal ion ($Ca^{2+}$, $Mg^{2+}$) is bound in an octahedral coordination by two phosphate oxygens of the TPP, the side chains of Asp157 and Asn187, the main chain oxygen of residue 189, and a water molecule. This coordination is very well conserved in pyruvate oxidase, pyruvate decarboxylase (PDC), transketolase, and benzoylformate decarboxylase (BFD) as well.[3] However, one of the few conserved interactions of the pyrimidine ring is the hydrogen bond between the side chain of Glu418 and the N(1′) atom.[3] It was suggested that the latter hydrogen bond activates the 4′-$NH_2$ group to act as an efficient proton acceptor for the C(2) proton, initializing in this way the catalytic cycle,[1d,3,5] because the adopted V conformation brings the 4′-$NH_2$ close to C(2). Our recent studies, supporting the previous suggestion, showed that a TPP−metal complex with a direct N(1′)−metal bond does not present cocatalytic activity.[6] This N(1′)−metal bond may act as an inhibitor preventing the hydrogen bond formation between the N(1′) atom and the side chain of Glu418 and, therefore, preventing the 4′-$NH_2$ from acting as a proton acceptor for the C(2) proton.[6]

The catalytic mechanisms of TPP-dependent enzymes are dominated by the chemistry of the TPP cofactor and its intermediates. Thus, the interactions of active aldehyde deriva-

[†] Department of Chemistry.
[‡] Department of Environmental and Natural Resources Management.

(1) (a) Schellenberg, A. *Angew. Chem., Int. Ed. Engl.* **1967**, *6*, 1024. (b) Kluger, R. *Chem. Rev.* **1987**, *87*, 863. (c) Kluger, R. *Pure Appl. Chem.* **1997**, *69*, 1957. (d) Schellenberger, A. *Biochim. Biophys. Acta* **1998**, *1385*, 177.
(2) Pletcher, J.; Sax, M.; Blank, G.; Wood, M. *J. Am. Chem. Soc.* **1977**, *99*, 1396.
(3) (a) Muller, Y. A.; Schulz, G. E. *Science* **1993**, *259*, 965. (b) Dyda, F.; Furey, W.; Swaminathan, S.; Sax, M.; Farrenkopf, B.; Jordan, F. *Biochemistry* **1993**, *32*, 6165. (c) Lindqvist, Y.; Schneider, G.; Ermler, U.; Sundstrom, M. *EMBO J.* **1992**, *11*, 2373. (d) Nikkola, M.; Lindqvist, Y.; Schneider, G. *J. Mol. Biol.* **1994**, *238*, 387. (e) Hasson, M. S.; Muscate, A.; McLeish, M. J.; Polovnikova, L. S.; Gerlt, J. A.; Kenyon, G. L.; Petsko, G. A.; Ringe, D. *Biochemistry* **1998**, *37*, 9918.
(4) Louloudi, M.; Hadjiliadis, N. *Coord. Chem. Rev.* **1994**, *135*, 429 and references therein.
(5) Kern, D.; Kern, G.; Neef, H.; Tittmann, K.; Killenberg-Jabs, M.; Wikner, C.; Schneider, G.; Hübner, G. *Science* **1997**, *275*, 67.
(6) Malandrinos, G.; Louloudi, M.; Koukkou, A. I.; Sovago, I.; Drainas, K.; Hadjiliadis, N. *J. Biol. Inorg. Chem.* **2000**, *5*, 218.

10.1021/ic001465t CCC: $20.00 
Published on Web 08/03/2001

**Scheme 1**

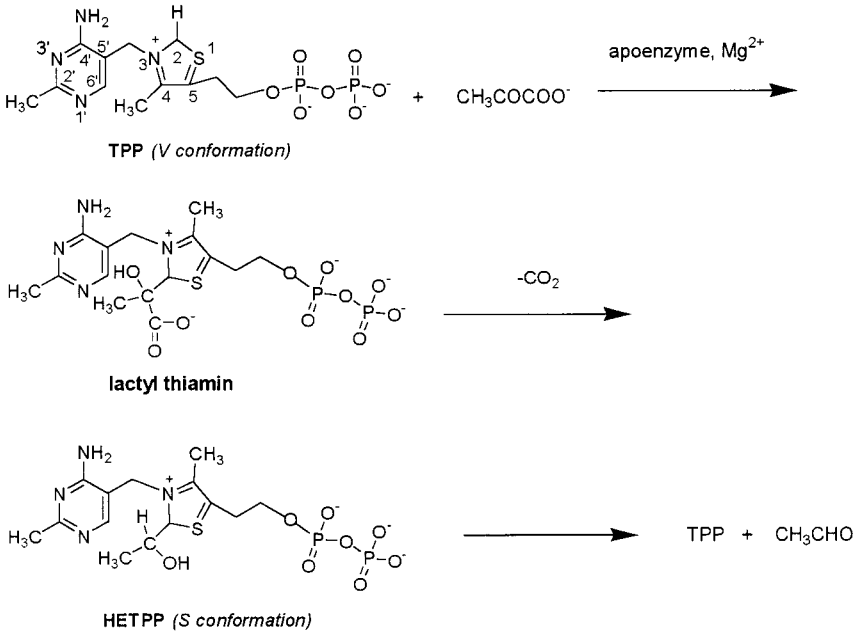


tives of thiamin, 2-(α-hydroxybenzyl)- and 2-(α-hydroxy-α-cyclohexylmethyl)thiamin, with group IIB metals,[7a] as well as with first row transition metals,[7b] are of particular interest. In all of these cases, the metal ions were found to be coordinated to the N(1′) atom of the pyrimidine moiety.[7a,b] When the active aldehyde pyrophosphate derivatives of thiamin, 2-(α-hydroxybenzyl)- and 2-(α-hydroxyethyl)thiamin pyrophosphate (HETPP), were used as ligands, metal coordination both to the pyrimidine N(1′) and to the pyrophosphate group was detected.[7c,d] Exceptionally, $Hg^{2+}$ forms complexes with the active aldehyde pyrophosphate derivatives of thiamin coordinated only to N(1′).[7e]

Recently, in order to evaluate the coenzyme activity of HETPP−metal complexes, we have performed enzymic studies using the pyruvate decarboxylase (PDC) apoenzyme.[6] These studies showed that HETPP−metal complexes which hold the S conformation and present direct metal−$N_{1'}$ and metal−pyrophosphate oxygen bonds can exhibit coenzyme activity.[6] It appears therefore that the "active aldehyde" intermediates prefer the S conformation which, in this catalytic step, does not inhibit the enzymic procedure. In this context, it is noteworthy that free exogenous HETPP also shows the same coenzyme activity.[8]

Despite the numerous crystallographic data[3,4,7a,c,e] and some molecular modeling studies,[9] structural information on the active site of thiamin-dependent enzymes *in solution* is missing. For this reason, we decided to construct and characterize a $Cu^{2+}$−thiamin−substrate−peptide system in solution. In this context, we have synthesized (a) the pentapeptide Asp-Asp-Asn-Lys-Ile which mimics the metal binding site Asp185-Asp186-Asn187-Lys188-Ile189 of transketolase and surrounds the pyrophosphate moiety[3c,d] and (b) the HETPP, because the C(2) atom of TPP forms a covalent adduct with the substrate, a mechanism common to all TPP-catalyzed reactions, leading to HETPP. Finally, here we present the study of the tertiary $Cu^{2+}$−pentapeptide−2-(α-hydroxyethyl)thiamin pyrophosphate in solution. These data provide information on the coordination environment of copper(II) in $Cu^{2+}$−HETPP, $Cu^{2+}$−pentapeptide, and $Cu^{2+}$−pentapeptide−HETPP systems as a function of pH. Furthermore, the adopted thiamin conformation is explored. These results can refer directly to thiamin catalysis, because the protein pocket around the pyrophosphate group and both thiamin and the metal cofactors, as well as the substrate, are present.

## Experimental Section

**Materials.** Thiamin pyrophosphate was purchased from Sigma Chemical Co. and used without further purification. $CuCl_2$ and all other chemicals used were from Aldrich AG. The protected amino acids Fmoc-Asp(OBu$^t$)-OH, Fmoc-Asn-OH, Fmoc-Lys(Boc)-OH, and Fmoc-Ile-OH and the resin 2-chlorotrityl chloride were purchased from CBL Chemicals Ltd. (Patras-Greece).

**Synthesis of the Compounds. Preparation of the Ligand 2-(α-Hydroxyethyl)thiamin Pyrophosphate (HETPP) Chloride.** 2-(α-Hydroxyethyl)thiamin pyrophosphate chloride was prepared according to the literature.[10] The ligand forms, $(HETPPH_2)^0$ (neutral ylide) or $(HETPPH)^-K^+$, were obtained by addition of 1 or 2 equiv of 0.1 N KOH in alcoholic solutions. Any insoluble material was removed prior to use.

**$[Cu^{II}(HETPPH)Cl\cdot 3H_2O]_n$.** This complex was prepared by mixing equimolar amounts of $(LH)^-K^+$ and the cupric chloride in a 1:1 solution by volume of methanol and ethanol. The reaction mixture was stirred overnight at room temperature, and the resulting precipitate was isolated and analyzed. Anal. Calcd for $[Cu^{II}(HETPPH)Cl\cdot 3H_2O]_n$ ($C_{14}H_{27}N_4O_{11}P_2SClCu$, where $n = 1$): C, 28.34%; H, 4.08%; N, 9.44%; S, 5.40%; Cu, 10.71%. Found: C, 28.37%; H, 3.97%; N, 9.27%; S, 5.16%; Cu, 10.60%. Mp 155−157 °C (dec). IR (KBr, $cm^{-1}$): 1657, 1624, pyrimidine ring (8a) + $\delta(NH_2)$; 1541, pyrimidine ring (8b); 1210, $\nu$(P═O); 1092, 1058, $\nu$(C−O) + $\nu$(P−O−C); 1003, 927, $\nu$(P−O) + $\nu$(P−O−P); 553, $\delta$(P−O); 298, $\nu$(Cu−Cl); 276, $\nu$(Cu−N).[7c] $^1$H NMR

(7) (a) Louloudi, M.; Hadjiliadis, N.; Feng, J. A.; Sukumar, S.; Bau, R. J. *J. Am. Chem. Soc.* **1990**, *112*, 7233. (b) Louloudi, M.; Hadjiliadis, N. *J. Chem. Soc., Dalton Trans.* **1992**, 1635. (c) Malandrinos, G.; Louloudi, M.; Mitsopoulou, C. A.; Butler, I. S.; Bau, R.; Hadjiliadis, N. *J. Biol. Inorg. Chem.* **1998**, *3*, 437. (d) Dodi, K.; Louloudi, M.; Malandrinos, G.; Hadjiliadis, N. *J. Inorg. Biochem.* **1999**, *73*, 41. (e) Dodi, K.; Gerothanassis, I.; Hadjiliadis, N.; Schreiber, A.; Bau, R.; Butler, I. S.; Barrie, P. *Inorg. Chem.* **1996**, *35*, 6513.

(8) Kluger, R.; Trachsel, M. R. *Bioorg. Chem.* **1990**, *18*, 136.

(9) (a) Shin, W.; Oh, D. G.; Chae, C. H.; Yoon, T. S. *J. Am. Chem. Soc.* **1993**, *115*, 12238. (b) Lobell, M.; Crout, D. H. G. *J. Am. Chem. Soc.* **1996**, *118*, 1867.

(10) (a) For preparation of the ligand, see ref 7c and references therein. (b) Shin, W.; Pletcher, J.; Blank, G.; Sax, M. *J. Am. Chem. Soc.* **1977**, *99*, 3491.

**Table 1.** Stability Constants (log $\beta$)[a] and Electronic and EPR Spectral Parameters of the $Cu^{2+}$−HETPP System

| pH | major species | log $\beta$ | $\lambda_{max}$ (nm) | $\epsilon$ ($dm^{-3}$ mol $cm^{-1}$) | $g_{\|\|}$ | $A_{\|\|}$ (G) | $g_{\perp}$ | $A_{\perp}$ (G) |
|---|---|---|---|---|---|---|---|---|
| 3.0 | | | 808 | 18.8 | 2.315 | 129 | 2.009 | 14 |
| 4.1 | $[M_2A_2H_2]^{2+}$ | 23.33(4) | 797 | 25.8 | | | | |
| 5.0 | $[M_2A_2H]^{+}$ | 8.65(4) | 787 | 32.8 | | | | |
| 6.5 | $[M_2A_2]^{0}$ | 13.70(3) | 779 | 60.0 | 2.248 | 145 | 2.002 | 14 |

[a] $T$ = 298 K; $I$ = 0.2 mol $dm^{-3}$ (KCl); $[Cu^{2+}]$ = [HETPP] = 4 mM.

($D_2O$, $\delta$): 7.8, C(6′)−H (v br); 5.9, $CH_2$(3,5′); 5.6, C(2a)−H; 4.35, $CH_2$(5b) (br); 3.5, $CH_2$(5a); 2.55, C(4)−$CH_3$; 2.7, C(2′)−$CH_3$ (br); 1.85, C(2a)−$CH_3$. The resonance of C(6′)−H adjacent to N(1′) is the one most affected by Cu(II). It is broadened ($\Delta W_{1/2}$ = 144 Hz) and shifted by 0.6 ppm downfield compared to that of the free ligand $(HETPPH)^{-}K^{+}$ at concentrations of 5 mM $[Cu^{II}(HETPP)Cl\cdot 3H_2O]_n$. $^{31}P$ NMR: the resonances of $P_\alpha$ and $P_\beta$ atoms are completely lost at concentrations of 5 mM $[Cu^{II}(HETPP)Cl\cdot 3H_2O]_n$. EPR (powder): $g_{||}$ = 2.29, $g_{\perp}$ = 2.05, $A_{||}$ = 161 G, $A_{\perp}$ = 25 G.

**Peptide Synthesis.** The peptide Asp-Asp-Asn-Lys-Ile was synthesized by solid-phase peptide synthesis using the 2-chlorotrityl chloride resin (substitution 1.1−1.6 mequiv $g^{-1}$) as the solid support.[11a] The standard Fmoc procedure was used.[11b,c] The Fmoc group was used for temporary protection of the amino group, and 1-hydroxybenzotriazole (HOBt) and dicyclohexylcarbodiimide (DCC) were used as coupling reagents. The peptide was cleaved from the resin by a mixture of $CH_3COOH/CF_3CH_2OH/CH_2Cl_2$ (1:2:7 v/v). The peptide was purified by flash chromatography using silica gel as column packing material and the solvent mixture $CH_3CN/H_2O$ (5:1 v/v). The $Bu^t$ and Boc protecting groups of the side chains were removed by a solution of 1.2 N HCl/$CH_3COOH$ after the purification of the peptide. Peptide purity was controlled by TLC in the systems $CH_3CN/H_2O$ (5:1 v/v) and BuOH/$CH_3COOH/H_2O$ (4:1:1 v/v).

**Methods. Far IR and Mid-IR Spectra.** The IR spectra in the region 4000−50 $cm^{-1}$ were recorded on a Perkin-Elmer Spectrum GX SP-IR system.

**UV−vis spectra** were recorded using a UV/VIS/NIR JASCO spectrophotometer.

**EPR Spectra.** Continuous-wave (CW) EPR spectra were recorded at liquid helium temperatures with a Bruker ER 200D X-band spectrometer equipped with an Oxford Instruments cryostat. The microwave frequency and the magnetic field were measured with a microwave frequency counter HP 5350B and a Bruker ER035M NMR−gaussmeter, respectively. Experimental conditions: microwave power, 20 mW; modulation amplitude, 12 G; temperature of the EPR experiments, 15 K.

**One- and Two-Dimensional NMR Spectra.** All NMR spectra were obtained at room temperature (25 ± 1 °C) in a Bruker AMX-400 MHz spectrometer in a solution of $D_2O/H_2O$ (1:4 v/v) using TMS as an external reference. $^1H$ NMR and $^{13}C$ NMR spectra were recorded at 400 and 100.58 MHz, respectively, in concentrations of 5 mM for $^1H$ NMR and TOCSY spectra and of 50−100 mM for $^{13}C$ NMR spectra. The usual $^1H$ spectrometer conditions consisted of 8064 Hz sweep width, 64 scans, and 1 K data points. For 2D $^1H$ NMR spectrum TOCSY, 256 $t_1$ increments were accumulated into 1 K data points with 32 scans each. The evolution time after the first 90° pulse was 1.0 s, while the acquisition time was typically 0.1 s. The MLEV-17 pulse sequence (50 ms) was used for mixing in the TOCSY experiment.[12a] The initial 256 × 1024 data matrix was zero filled and multiplied by a sine-bell function in both $t_1$ and $t_2$ dimensions prior to Fourier transformation. Phase-sensitive $^1H-^{13}C$ HMQC (heteronuclear multiple quantum coherence)[12b] and $^1H-^{13}C$ HMBC (heteronuclear multiple bond coherence)[12c] spectra were recorded at 25 ± 1 °C with $t_{1(max)}$ = 55.1 ms and $t_2$ = 457 ms for HMQC and $t_{1(max)}$ = 22 ms and $t_2$ = 209 ms for HMBC experiments.

**Stability Constant Measurements.** Stability constant measurements of the copper complexes were determined potentiometrically, using a Radiometer PHM 84 pH meter equipped with a 6.0234.100 combined electrode (Metrohm) and a DOSIMAT 715 automatic buret (Metrohm) containing carbonate-free potassium hydroxide in known concentrations. The final model chosen, which gave the best fit, included the $M_2L_2H_2$, $M_2L_2H$, and $M_2L_2$ species (where M = Cu(II) and L = ligand). The pH-metric titrations were performed on 10 mL samples in the concentration range 1 × $10^{-3}$−4 × $10^{-3}$ mol $dm^{-3}$ at metal ion-to-ligand ratios between 1:1 and 4:1. Argon was bubbled through the samples to ensure the absence of oxygen and to stir the solutions. All measurements were carried out at 298 K and at a constant ionic strength of 0.2 mol $dm^{-3}$ KCl. The pH-metric data were evaluated by the PSEQUAD computer program.[13]

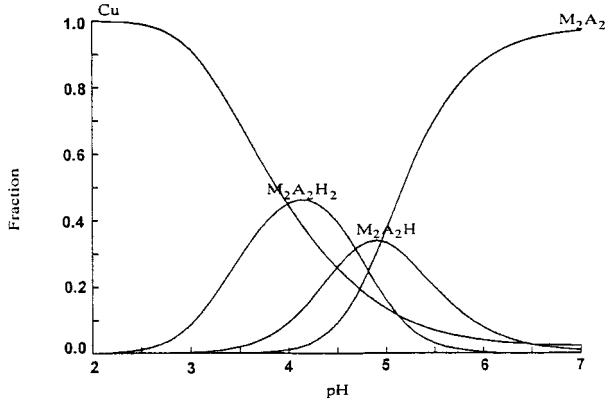


**Figure 1.** Species distribution diagram of the $Cu^{2+}$−HETPP system ($T$ = 298 K; $I$ = 0.2 mol $dm^{-3}$ (KCl); $[Cu^{2+}]$ = [HETPP] = 4 mM).

## Results and Discussion

**$Cu^{2+}$−HETPP.** The stability constants (log $\beta$) (eqs 1 and 2) for the Cu(II) complex of HETPP appear in Table 1.The species distribution of complexes formed in the $Cu^{2+}$−HETPP system is shown in Figure 1.

$$2M^{2+} + 2(HETPP)^{-} + nH^{+} \Leftrightarrow [M_2(HETPP)_2H_n]^{(2+n)} \quad (1)$$

$$K[(M_2(HETPP)_2H_n)^{(2+n)}] = [(M_2(HETPP)_2H_n)^{(2+n)}]/[M^{2+}]^2[(HETPP)^{-}]^2[H^{+}]^n \quad (2)$$

The titration curves can be fitted by assuming the formation of dimeric metal complexes of the type $[Cu(HETPPH)]_2$. This is in agreement with the previously reported $[M(HETPPH)]_2$ metal complexes (where M = Zn(II), Cd(II)).[7c] From Figure 1, it is seen that the formation of the $[M_2(HETPP)_2H_2]^{2+}$ complex species occurs between pH 2.5 and 5.5 and the formation of $[M_2(HETPP)_2H]^{+}$ occurs between pH 3.5 and 6.5. At pH > 6.5, the $[M_2(HETPP)_2]^{0}$ species predominates. Generally, HETPP forms a more stable complex species with Cu(II) ions than with Cd(II) and Zn(II).[14]

(11) (a) Barlos, K.; Chatzi, O.; Gatos, D.; Stavropoulos, G. *Int. J. Pept. Protein Res.* **1991**, *37*, 513. (b) Stavropoulos, G.; Karagiannis, K.; Vynios, D.; Papaioannou, D.; Aksnes, D. W.; Froystein, N. A.; Francis, G. W. *Acta Chem. Scand.* **1991**, *45*, 1047. (c) Carpino, L. A. *Acc. Chem. Res.* **1987**, *20*, 401.

(12) (a) Davis, D. G.; Bax, A. *J. Am. Chem. Soc.* **1985**, *107*, 2821. (b) Bax, A.; Subramanian, S. J. *J. Magn. Reson.* **1986**, *67*, 565. (c) Bax, A.; Summers, M. F. *J. Am. Chem. Soc.* **1986**, *108*, 2093.

(13) Zékàny, L.; Nagypàl, I. In *Computational Methods for the Determination of Stability Constants*; Leggett, D. J., Ed.; Plenum: New York, 1991.

(14) $\beta_{Cu^{2+}-HETPP}/\beta_{Cd^{2+}-HETPP}$ = 234; $\beta_{Cu^{2+}-HETPP}/\beta_{Zn^{2+}-HETPP}$ = 490.

**Table 2.** Stability Constants (log $\beta$) and Deprotonation Constants (p$K$) for Proton Complexes of Asp-Asp-Asn-Lys-Ile ($T$ = 298 K; $I$ = 0.2 mol $dm^{-3}$ (KCl))

| $H_5A$ | | $H_4A$ | | $H_3A$ | | $H_2A$ | | HA | |
|---|---|---|---|---|---|---|---|---|---|
| log $\beta$ | p$K_1$ (carboxylic group) | log $\beta$ | p$K_2$ (carboxylic group) | log $\beta$ | p$K_3$ (carboxylic group) | log $\beta$ | p$K_4$ ($Asp^1-NH_2$) | log $\beta$ | p$K_5$ (Lys-$\epsilon$-$NH_2$) |
| 28.17(8) | 2.82 | 25.36(4) | 3.46 | 21.89(6) | 3.81 | 18.09(3) | 7.72 | 10.36(1) | 10.38 |

The $P_\beta-OH$ group of the terminal phosphorus is protonated in both of the ligand molecules in the species $[M_2(HETPP)_2H_2]^{2+}$. On increasing the pH, the $P_\beta-OH$ of the first ligand of the dimers is very probably deprotonated, corresponding to the $[M_2(HETPP)_2H]^+$ species. The deprotonation of the $P_\beta-OH$ of the second ligand occurs at a slightly higher pH, resulting in the $[M_2(HETPP)_2]^0$ species, whose concentration reaches a maximum around physiological pH. Such a deprotonation cannot be followed closely by vis and EPR spectroscopies, because the $P_\beta-OH$ group of the terminal phosphorus is not coordinated to a copper ion. From Figure 1, we infer that at pH 3.0 the $[M_2(HETPP)_2H_2]^{2+}$ is the only species present, though in low concentration. Its d−d transition band is centered at 808 nm, and the EPR parameters are $g_{||} = 2.315$, $g_\perp = 2.009$, $A_{||} = 129$ G, and $A_\perp = 14$ G. At pH 5, the $[M_2(HETPP)_2H]^+$ species coexists with $[M_2(HETPP)_2H_2]^{2+}$ and $[M_2(HETPP)_2]^0$. However, at pH 6.5, $[M_2(HETPP)_2]^0$ is the major species ($f \sim 100\%$) with spectral features of $\lambda_{max} = 779$ nm, $g_{||} = 2.248$, $g_\perp = 2.002$, $A_{||} = 145$ G, and $A_\perp = 14$ G.

In the $^1H$ NMR spectrum of the $[M_2(HETPP)_2]^0$ species at pH 6.5 ($[Cu^{2+}] = 3.9 \times 10^{-2}$ mM; [HETPP] = 2 mM in $D_2O$ solution), the resonance of C(6′)−H adjacent to N(1′) is the one most affected by Cu(II). It is broadened ($\Delta W_{1/2} = 144$ Hz) and shifted by 0.6 ppm downfield compared to the resonance of the free ligand $(HETPPH)^-K^+$. The signal of $^bCH_2$ is broadened with $\Delta W_{1/2} = 48$ Hz as well as the resonance of C(2′)−$CH_3$. In the last case, the $\Delta W_{1/2}$ is not detected because of a partial overlap between the C(2′)−$CH_3$ and C(4)−$CH_3$ signals. In the $^{31}P$ NMR spectrum, the resonances of the $P_\alpha$ and $P_\beta$ atoms are completely lost. These NMR data provide evidence that the Cu(II) is coordinated to the pyrophosphate group and to the pyrimidine N(1′) site.

On going from pH 3.0 to pH 6.5, the ∼29 nm blue shift of the d−d transition with a subsequent decrease in the $g_{||}$ value and a concomitant increase in $A_{||}$ (Table 1) suggests increased ligand field strength; this is due to the deprotonation of the $P_\beta-OH$ group which localizes another anionic charge in the vicinity of the metal center. Signals attributed to binuclear species with a copper−copper interaction have not been detected by EPR in any case. Moreover, pulsed EPR data for $[M_2(HETPP)_2]^0$ around physiological pH strongly suggested that the copper atom was coordinated by two phosphate oxygens of the pyrophosphate group and the N(1′) atom of the pyrimidine moiety of HETPP.[15]

**Peptide Asp-Asp-Asn-Lys-Ile**. The $^1H$ NMR and $^{13}C$ NMR chemical shift data together with the assignments of the free peptide resonances are given in the Supporting Information. These assignments were made by two-dimensional $^1H-^1H$ TOCSY, $^1H-^{13}C$ HMQC, and $^1H-^{13}C$ HMBC spectral analysis (Supporting Information).

The stability constants and the p$K$ values of the proton complexes of the oligopeptide appear in Table 2, while the species distribution curves are displayed in Figure 2. The pentapeptide Asp-Asp-Asn-Lys-Ile contains five groups that can be deprotonated over the pH range studied here. These are three

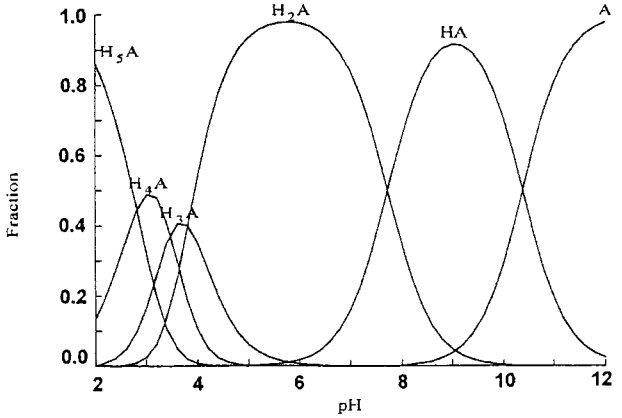


**Figure 2.** Species distribution diagram of the pentapeptide Asp-Asp-Asn-Lys-Ileu ($T$ = 298 K; $I$ = 0.2 mol $dm^{-3}$ (KCl)).

**Chart 1**

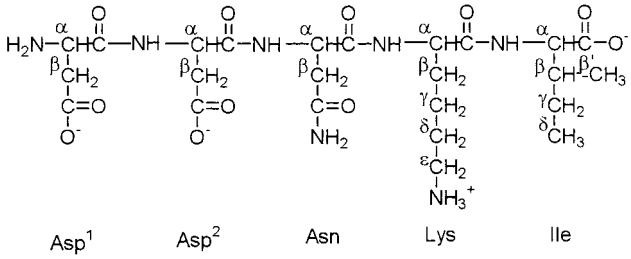


carboxylate groups and two amino groups (Chart 1). At low pH, the protonation equilibria corresponding to the protonation of the carboxylate groups will be macroconstants with contributions from all three protonation equilibria. The stepwise constants cannot, therefore, be assigned to protonation of any particular carboxylate oxygen, that is, $Asp^1-COO^-$, $Asp^2-COO^-$, or Ile−$COO^-$. In slightly alkaline solutions, the ammonium terminal ($Asp^1-NH_2$) loses one proton, and finally at higher pH values, deprotonation of the Lys-$\epsilon$-$NH_2$ ammonium group takes place.

**$Cu^{2+}$−Asp-Asp-Asn-Lys-Ile.** In this section, the vis and the CW EPR spectra at various pH values are compared with the speciation behavior in order to probe the solution structure of the $Cu^{2+}$−peptide system. The resulting stability constants as well as the visible and EPR spectroscopic data are summarized in Table 3. The species distribution diagrams of this system are shown in Figure 3, while selected EPR spectra appear in Figure 4.

Previous studies of $Cu^{2+}$ complexes with peptides have established an empirical formula which can be used as a diagnostic tool for predicting the $\lambda_{max}$ of the d−d band.[16] The energy of the d−d transition can be expressed as the sum of the individual contributions from the four donor atoms lying in the equatorial plane around the $Cu^{2+}$ atom. The contribution from amine nitrogens is considerably higher than that from oxygens.[16] Thus, substitution of a nitrogen for an oxygen in

(15) Malandrinos, G.; Louloudi, M.; Deligiannakis, Y.; Hadjiliadis, N. *J. Phys. Chem. B*, in press.

(16) (a) Billo, E. J. *Inorg. Nucl. Chem. Lett.* **1974**, *10*, 613. (b) Stephens, A. K. W.; Orvig, C. *J. Chem. Soc., Dalton Trans.* **1998**, 3049.

**Table 3.** Stability Constants (log $\beta$)[a] and Electronic and EPR Spectral Parameters of the $Cu^{2+}$−Peptide Complex

| pH | major species | log $\beta$ | $\lambda_{max}$ (nm) | $\epsilon$ ($dm^{-3}$ mol $cm^{-1}$) | $g_{\|\|}$ | $A_{\|\|}$ (G) | $g_{\perp}$ | $A_{\perp}$ (G) |
|---|---|---|---|---|---|---|---|---|
| 4.6 | MAH | 17.07(6) | 637 | 47 | 2.27 | 193 | 2.09 | 30 |
| 6.4 | MA | 12.68(4) | 630 | 71 | 2.22 | 195 | 2.08 | 30 |
| 9.0 | $MAH_{-1}$ | 4.32(8) | 560 | 103 | 2.18 | 215 | 2.03 | 20 |
| 10.0 | $MAH_{-2}$ | −5.06(7) | 529 | 114 | 2.14 | 229 | 2.00 | 12 |
| 11.0 | $MAH_{-3}$ | −15.33(8) | 521 | 117 | 2.14 | 229 | 2.00 | 12 |

[a] $T$ = 298 K; $I$ = 0.2 mol $dm^{-3}$ (KCl); [$Cu^{2+}$] = [peptide] = 4 mM.

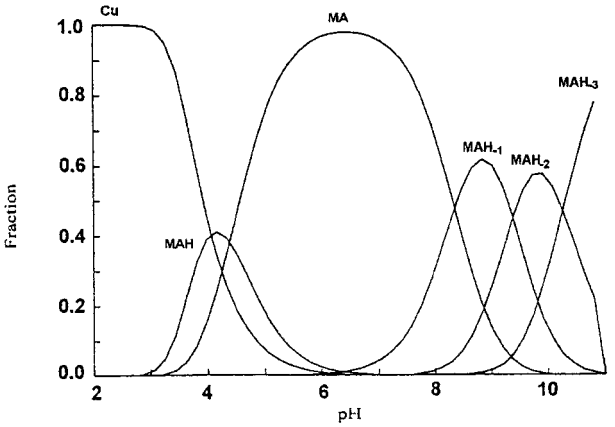


**Figure 3.** Species distribution diagram of the $Cu^{2+}$−Asp-Asp-Asn-Lys-Ileu system ($T$ = 298 K; $I$ = 0.2 mol $dm^{-3}$ (KCl); [$Cu^{2+}$] = [peptide] = 4 mM).

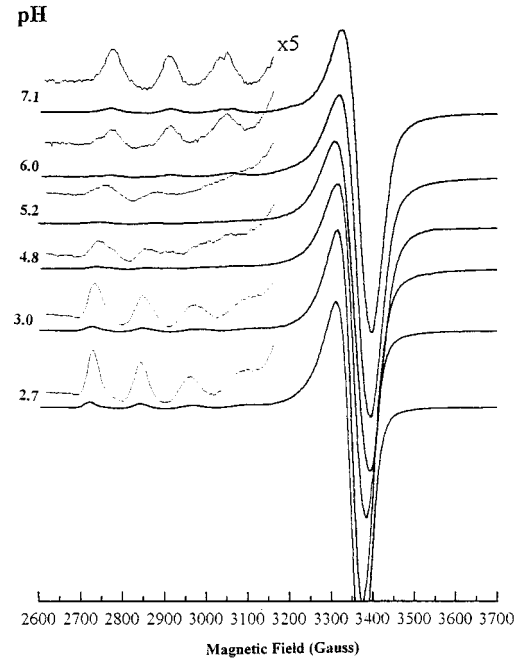


**Figure 4.** CW EPR spectra of the $Cu^{2+}$−Asp-Asp-Asn-Lys-Ileu system as a function of pH.

the equatorial sites causes a decrease in $\lambda_{max}$ (axial donor atoms have a minor effect, causing a slight increase in $\lambda_{max}$).[16]

Concerning now the coordination behavior of Asp to copper(II), it is known that the N-terminal Asp residue significantly stabilizes the copper(II) complex with only one nitrogen atom coordinated (1N) as a result of chelation through the $\beta$-carboxylate group, rather than through the peptide C═O oxygen.[17] Aspartic acid residues in the second or third position of the peptide sequence stabilize 2N and 3N complexed species, respectively, significantly delaying and, in some cases, completely preventing formation of 4N complexes.[17] As a result, the positions of Asp residues in a peptide chain have a significant influence on copper(II) interactions in solution with the peptides containing Asp residues. For example, the presence of an Asp residue in the $x$ position in a peptide chain blocks the involvement of the effective nitrogen donor of the $x$ peptide bond with subsequent Cu−$N^-$coordination. Thus, for complexes involving $x + 1$ nitrogens ($x + 1$ N), coordination could not be detected in such systems.[18] A quantitative indication of the stabilizing effect of the peptides containing Asp residues may be obtained by simple comparison of log $\beta$ values. As a result, the species distribution curves for the major species of peptides containing Asp residues have wide ranges of existence compared to those without Asp residues. Thus, in our case, the interaction of $Cu^{2+}$ with Asp-Asp-Asn-Lys-Ile, which contains two Asp residues in the first and second positions, should result in a facile deprotonation of the first peptide bond supported by Cu−carboxylate binding ($Asp^1$−$COO^-$, $Asp^2$−$COO^-$) and should prevent the deprotonation of the other peptides bonds.

**A. MAH Species.** In potentiometric titrations for [Cu] = [peptide] = 4 mM, five $MAH_r$ species were detected, that is, MAH, MA, $MAH_{-1}$, $MAH_{-2}$, and $MAH_{-3}$ (Figure 3); M and A denote $Cu^{2+}$ and Asp-Asp-Asn-Lys-Ile, respectively. Formation of $Cu^{2+}$−hydroxyl species in the pH range 2−11 is not detected by spectroscopic data because of the enhanced stability of the formed species. The titration curves can be fit by assuming the formation of MAH species between pH 3.0 and 6.0. In this pH range, the spectroscopic data are $\lambda_{max}$ = 637 nm, $g_{||}$ = 2.27, $g_{\perp}$ = 2.09, $A_{||}$ = 193 G, and $A_{\perp}$ = 30 G. MAH species formation indicates coordination of the terminal amino group ($Asp^1$—$NH_2$), of the $\beta$−carboxylate of the $Asp^1$ residue ($Asp^1$—$COO^-$), and probably of the C═O peptide group of the $Asp^1$ (Chart 2). In this way, the amino group, which can form a six-membered chelate group with the copper and the $^-OOC^{\beta}$—$Asp^1$, anchors the metal ion supported by peptide C═O ($Asp^1$) binding, which stabilizes a five-membered chelate group. At 3.2 < pH < 10.0, the MA species predominates, and the MAH species is also present in the pH range 3.2−6.0. Complexes with 1N coordination have an absorption band in the 700−730 nm region, but it is of low intensity and is normally obscured when the concentration is low or when 2N complexes are also present.[17] As a result, the spectroscopic data in our case are the average of those of MAH (1N coordination) and MA (2N coordination) complexes.

**B. MA Species.** It should be renoted that MA species with 2N coordination are the major species in the pH range 3.2−10.0, reaching a maximum concentration at pH 6.0 ($f \sim 96\%$); stabilization of these complexes would therefore result in a widening of this band of stability. Such a broadening, though less extended, was found also with Ala-Asp-Ala-Asp (pH 5−9.5), Ala-Asp-Asp-Ala (pH 5−7.3), and Asp-Asp-Asp (pH

(17) Galey, J.-F.; Decock-Le Reverend, B.; Lebkiri, A.; Pettit, L. D.; Pyburn, S. I.; Kozlowski, H. *J. Chem. Soc., Dalton Trans.* **1991**, 2281.

(18) (a) Sovago, I.; Kiss, T.; Gergely, A. *Inorg. Chim. Acta* **1984**, *93*, L53. (b)Decock-Le Reverend, B.; Lebkiri, A.; Livera, C.; Pettit, L. D. *Inorg. Chim. Acta* **1986**, *124*, L19.

**Chart 2**

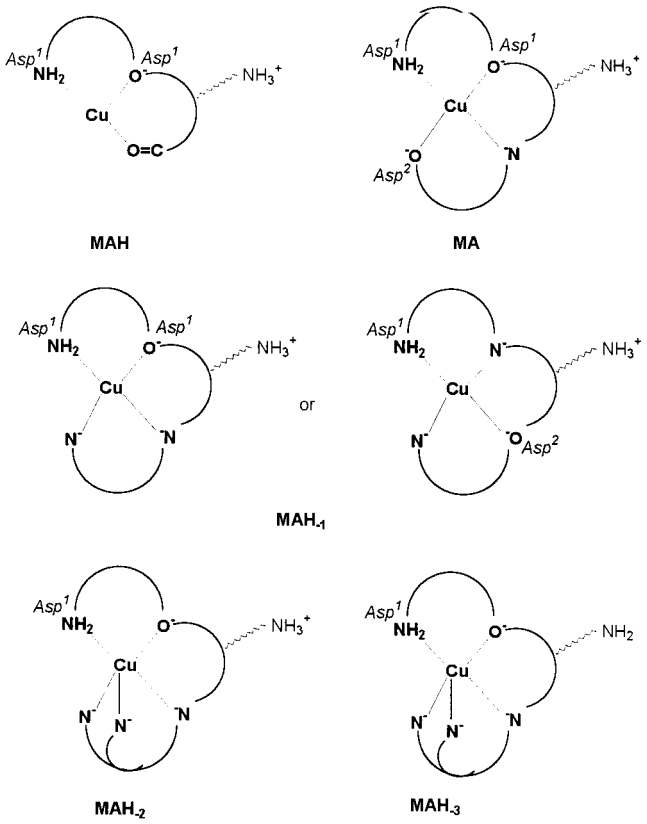


5−8).[17] Tridentate coordination in the MA species would involve binding of the terminal $NH_2$−Asp[1] group, of $^-OOC\beta$−Asp[1], of $^-OOC\beta$−Asp[2] carboxylates, and finally of a deprotonated peptide nitrogen $N^-$ (Chart 2). A p$K_a$ value of 4.55 is obtained for the deprotonation of the coordinated peptide $N^-$, which is comparable to the value of 4.8 for Asp-Asp-Asp for the formation of the same species, indicating facile formation and enhanced stability. From literature data, peptides which contain Asp residues and show the same mode of coordination present spectral features of $\lambda_{max} = 630-652$ nm, $g_{||} = 2.224-2.27$, and $A_{||} = 165-185$ G,[17] while Gly-Gly and $\beta$-Ala-Gly systems exhibit $\lambda_{max} = 622-658$ nm, $g_{||} = 2.220-2.271$, and $A_{||} = 152-203$ G.[19a] Comparison of our spectral data with the literature data indicates a high ligand field strength in this MA species supported by a slight decrease in $g_{||}$ and $\lambda_{max}$ and a concomitant increase in $A_{||}$. This presents a typical trend for increasing in-plane donor strength in tetragonally elongated copper complexes.[19] The increased ligand field is a result of the formation of a third chelate ring which further stabilizes the copper complex and also is a result of the increased total negative charge of the copper atom and its four close-lying ligand atoms. Putting our EPR parameters $g_{||}$ and $A_{||}$ on the diagrams of Peisach and Blumberg,[19b] we predict a coordination sphere containing two nitrogen atoms and two oxygen atoms with a minus one (−1) total charge for the copper and its four close-lying ligands in accordance with our suggestion ($NH_2$, $N^-$, and $2COO^-$ as donor set). Moreover, at this pH region, both terminal amino group and aspartate $\beta$-carboxylate coordination is strongly supported by pulsed EPR data.[15]

**C. MAH$_{-1}$ Species.** A second peptide NH deprotonation takes place at 6.5 < pH < 11.0, leading to a $MAH_{-1}$ species ($MA \leftrightarrow MAH_{-1} + H^+$) which reaches a maximum concentration at pH 9.0 ($f \sim 60\%$). A p$K_a$ of 8.32 is obtained for this deprotonation, which is comparable to the value of 8.37 found with Asp-Asp-Asp. Its d−d transition band (centered at 560 nm) indicates planar coordination of three nitrogen atoms and one oxygen atom, while the EPR parameters ($g_{||} = 2.18$, $g_\perp = 2.03$, $A_{||} = 215$ G, and $A_\perp = 20$ G) according to Peisach and Blumberg diagrams[19b] indicate a coordination mode with 3N and 1O and an overall charge of −1 (Chart 2). When the observed EPR parameters are compared with those from literature data for 3N, 1O coordination ($g_{||} = 2.20-2.24$, $A_{||} = 185-210$ G), it is seen that in our case the observed $g_{||}$ value and the concomitant increase in the $A_{||}$ value can be attributed to an increased ligand field strength.[19a]

**D. MAH$_{-2}$ Species.** Increasing basicity leads to the formation of $MAH_{-2}$ species ($MAH_{-1} \leftrightarrow MAH_{-2} + H^+$) with a maximum concentration at pH 10.0 ($f \sim 58\%$) and spectral features of $\lambda_{max} = 529$ nm, $g_{||} = 2.145$, and $A_{||} = 229$ G. The p$K_a$ value of 9.42 for this deprotonation is significantly higher than that of the corresponding species of $Gly_5$, which is 7.89. Spectral data taken from the literature[20] with $\lambda_{max} = 508-520$ nm, $g_{||} = 2.17-2.18$, and $A_{||} = 205-212$ G are attributed to $NH_2$ and $3N^-$ binding. In our case, the ∼9−19 nm red shift of the d−d transition of the $MAH_{-2}$ species compared to literature can be explained by assuming that one of the four nitrogen atoms coordinates to the metal ion in an axial position. The above-mentioned destabilization of the $MAH_{-2}$ species compared to that of the $Gly_5$ system is consistent with this hypothesis.[20] Moreover, large deviations from square planar coordination could shift $g_{||}$ to smaller values closer to $g = 2$,[19b] which further supports a $NH_2$, $3N^-$, and $COO^-$ coordination in the species in question with a nitrogen atom as an axial ligand (Chart 2). In such a case, the overall charge should be −2, and on the basis of the diagrams of Peisach and Blumberg,[19b] a coordination sphere with 3N and 1O or 4N can be suggested for the $MAH_{-2}$ species.

**E. MAH$_{-3}$ Species.** Spectral data for the $MAH_{-3}$ species are similar to those for the $MAH_{-2}$ species (Table 3), indicating a similar coordination environment. The p$K_a$ value of 10.27 for the deprotonation $MAH_{-2} \leftrightarrow MAH_{-3} + H^+$ is comparable to the pH value of deprotonation of the Lys-$\epsilon$-$NH_2$ ammonium group (10.38, see Table 2). Thus, the $MAH_{-3}$ species corresponds to the $MAH_{-2}$ one, showing the Lys-$\epsilon$-$NH_2$ group deprotonated (Chart 2). Finally, it is noted that, in all cases, the proposed structures in Chart 1 contain the L-members of the diastereomeric pairs.

**Tertiary $Cu^{2+}$−Peptide−HETPP System.** The interaction of $Cu^{2+}$ with Asp-Asp-Asn-Lys-Ile and HETPP has been studied first by potentiometric studies and then by vis and CW EPR spectroscopies. Given that the stability constants of the $Cu^{2+}$−peptide system are higher than those of $Cu^{2+}$−HETPP, the concentrations used in the tertiary system were $[Cu^{2+}] = [peptide] = 2$ mM and $[HETPP] = 4$ mM to favor the formation of tertiary species. The species distribution curves of this system and selected EPR spectra are depicted in Figures 5 and 6. Logarithmic stability constants, vis spectral data, and EPR parameters are given in Table 4.

In potentiometric titrations which have been accomplished at pH 8 to avoid thiamin hydrolysis, three $MACH_r$ tertiary

(19) (a) Sovago, I.; Sanna, D.; Dessi, A.; Varnagy, K.; Micera, G. *J. Inorg. Biochem.* **1996**, *63*, 99. (b) Peisach, J.; Blumberg, W. E. *Arch. Biochem. Biophys.* **1974**, *165*, 691.

(20) (a) Varnagy, K.; Sovago, I.; Agoston, K.; Liko, Z.; Suli-Vargha, H.; Sanna, D.; Micera, G. *J. Chem. Soc., Dalton Trans.* **1994**, 2939. (b) Torok, I.; Gajda, T.; Gyurcsik, B.; Toth, G. K.; Peter, A. *J. Chem. Soc., Dalton Trans.* **1998**, 1205. (c) Varnagy, K.; Szabo, J.; Sovago, I.; Malandrinos, G.; Hadjiliadis, N.; Sanna, D.; Micera, G. *J. Chem. Soc., Dalton Trans.* **2000**, 467.

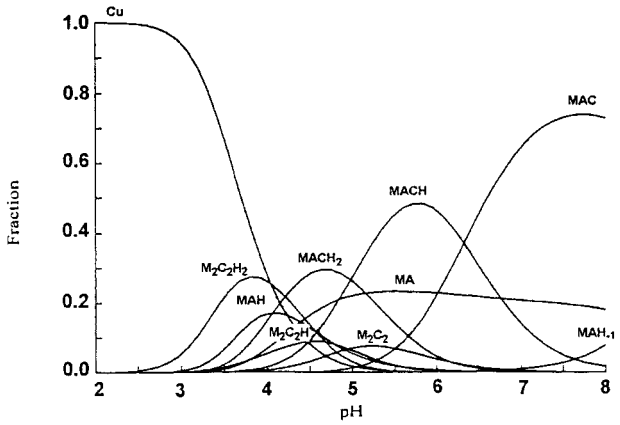


**Figure 5.** Species distribution diagram of the tertiary $Cu^{2+}$−peptide−HETPP system ($T$ = 298 K; $I$ = 0.2 mol $dm^{-3}$ (KCl); [$Cu^{2+}$] = [peptide] = 2 mM, [HETPP] = 4 mM).

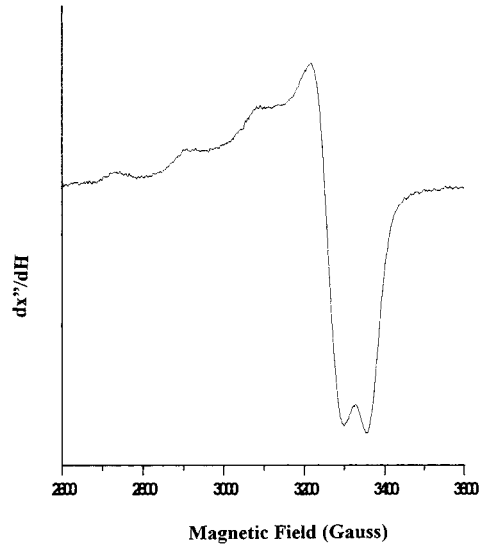


**Figure 6.** CW EPR spectrum of the $Cu^{2+}$−peptide−HETPP system at pH 7.2.

species were detected, that is, $MACH_2$, MACH, and MAC; M, A, and C denote $Cu^{2+}$, HETPP, and Asp-Asp-Asn-Lys-Ile, respectively. At pH < 4.5, $M_2C_2H_2$ is the major species, corresponding to the $[M_2(HETPPH)_2H_2]^{2+}$ complex with the $P_\beta$−OH group of the terminal phosphorus protonated in both ligand molecules of the dimers (see the stability constants of the $Cu^{2+}$−HETPP system). The species $[M_2(HETPPH)_2H]^+$ and $[M_2(HETPPH)_2]^0$ presented as $M_2C_2H$ and $M_2C_2$ in Figure 5 are formed as well, but at very low concentrations. Concerning the $Cu^{2+}$−peptide species complexes, the MAH coexists with $M_2C_2H_2$, $M_2C_2H$, MA, and the tertiary $MACH_2$ species (Figure 5), while the MA appears stable in a wide pH range, as expected on the basis of previous potentiometric data (see stability constants of $Cu^{2+}$−peptide system).

From stability constants and species distribution curves (Table 4, Figure 5), the tertiary $MACH_2$, MACH, and MAC species appear to have greater stability than the simpler $Cu^{2+}$−HETPP and $Cu^{2+}$−peptide systems. The formation of the above species has been accomplished at pH 4.6 ($f \sim 28\%$), 5.6 ($f \sim 42\%$), and 7.5 ($f \sim 70\%$), respectively.

**A. $MACH_2$ Species.** The $MACH_2$ shows $\lambda_{max}$ = 641 nm, $g_{||}$ = 2.29, $g_\perp$ = 2.08, $A_{||}$ = 195 G, and $A_\perp$ = 45 G. The value of $\lambda_{max}$ = 641 nm for $MACH_2$ suggests binding of the terminal $NH_2$ group and of a deprotonated peptide nitrogen $N^-$ as in the MA species ($\lambda_{max}$ = 630 nm). However, given that the value of $g_{||}$ = 2.29 is higher than that of $g_{||}$ for MA ($g_{||}$ = 2.22), a less distorted environment around the copper center probably is favored in the $MACH_2$ species; hence, there is a different mode of coordination. This could be consistent with the formation of only one chelate ring from a peptide environment, that is, the binding of a terminal $NH_2$−$Asp^1$ group and of a peptide $N^-$, instead of a tridentate coordination, as in the MA species, which involves additional coordination of $^-OOC^\beta$−$Asp^1$ and $^-OOC^\beta$−$Asp^2$ carboxylates. In the tertiary $MACH_2$ species, coordination of the thiamin pyrophosphate group is suggested instead of carboxylate binding (Chart 3).

**B. MACH Species.** Increasing basicity leads to the formation of the MACH species ($MACH_2 \leftrightarrow MACH + H^+$) with a maximum concentration at pH 5.6 ($f \sim 42\%$), a p$K$ value of 4.99 for this deprotonation, and a spectral feature of $\lambda_{max}$ = 637 nm. The small blue shift of the d−d transition of the MACH species can be explained by assuming that one nitrogen atom coordinates to the metal ion in an axial position, resulting in an elongated Cu−N bond (Chart 3).

**C. MAC Species.** The MAC species is the major one in the pH range 5.0−8.0 (end of titration), reaching its maximum concentration at pH 7.5 ($f \sim 70\%$). The existence of the tertiary MAC species around physiological pH is expected to have particular biological interest. With regard to the metal coordination environment, both peptide and thiamin binding must impose a distorted geometry. The coordination of thiamin pyrophosphate group and $N_{1'}$ is supported because of the formation of a macrochelate ring (Chart 3). On the other hand, bidentate coordination of peptide in MAC species would involve the binding of a terminal $NH_2$−$Asp^1$ group, of $^-OOC^\beta$−$Asp^1$ or $^-OOC^\beta$−$Asp^2$ carboxylates, and finally of a deprotonated peptide nitrogen $N^-$ (Chart 3). The d−d transition of this species (centered at 621 nm) and EPR parameters determined ($g_{||}$ = 2.22, $g_\perp$ = 2.025, $A_{||}$ = 203 G, and $A_\perp$ = 12 G) indicate 2N coordination into the equatorial plane as in the MA species ($g_{||}$ = 2.22, $A_{||}$ = 195 G). The ∼9 nm blue shift of the d−d transition of the MAC species compared to those of MA can be attributed as in the MACH species to the coordination of a N atom in an axial position, resulting in an elongated Cu−N bond. The structural model of the MAC species has also been supported by pulsed EPR data which demonstrate a copper coordination to phosphate oxygen atoms, to N(1′), and to the aspartate $\beta$-carboxylate.[15]

**D. $^1$H NMR.** In the $^1$H NMR spectrum of MAC at pH 7.2, the broadening of the signals of the protons close to the paramagnetic copper center has been used to assign the protons closer to the copper ion in the tertiary $Cu^{2+}$−peptide−HETPP system by comparison with the $^1$H NMR spectrum of the mixture peptide−HETPP. These spectra have been recorded at 298 K in $D_2O$ solution with a ratio of 1:50:100 for the tertiary $Cu^{2+}$−peptide−HETPP system ($(3.9 \times 10^{-2})$:2:4 mM) and with a ratio of 1:2 for the peptide−HETPP mixture. The signals originating from the HETPP molecule are easily observed in the peptide−HETPP $^1$H NMR spectrum. The interaction of Cu(II) with this mixture results in the broadening of the resonances of C(6′)−H and C(5b)$H_2$ of thiamin, which are the most affected. This interaction affects also the α-CH of $Asp^1$ and $\beta$-CH of $Asp^1$, $Asp^2$, and Asn protons to some extent. The above-mentioned observations are a good indication that the Cu(II) ion interacts with the N(1′) and the pyrophosphate moiety of HETPP as well as with the α-$NH_2$ and $\beta$-COOH groups of $Asp^2$.

A $^1$H−$^1$H ROESY spectrum of the tertiary $Cu^{2+}$−peptide−HETPP system has been recorded at 278 K (Figure 7).

**Table 4.** Stability Constants (log $\beta$)[a] and Electronic and EPR Spectral Parameters of the $Cu^{2+}$−Peptide−HETPP System

| pH | major species | log $\beta$ | $\lambda_{max}$ (nm) | $\epsilon$ ($dm^{-3}$ mol $cm^{-1}$) | $g_{\|\|}$ | $A_{\|\|}$ (G) | $g_{\perp}$ | $A_{\perp}$ (G) |
|---|---|---|---|---|---|---|---|---|
| 4.6 | $MACH_2$ | 27.22(9) | 641 | 51 | 2.29 | 195 | 2.08 | 45 |
| 5.6 | MACH | 22.23(7) | 637 | 63 | | | | |
| 7.5 | MAC | 15.90(9) | 621 | 82 | 2.22 | 203 | 2.025 | 12 |

[a] $T$ = 298 K; $I$ = 0.2 mol $dm^{-3}$ (KCl); [$Cu^{2+}$] = [peptide] = 2 mM, [HETPP] = 4 mM.

**Chart 3**

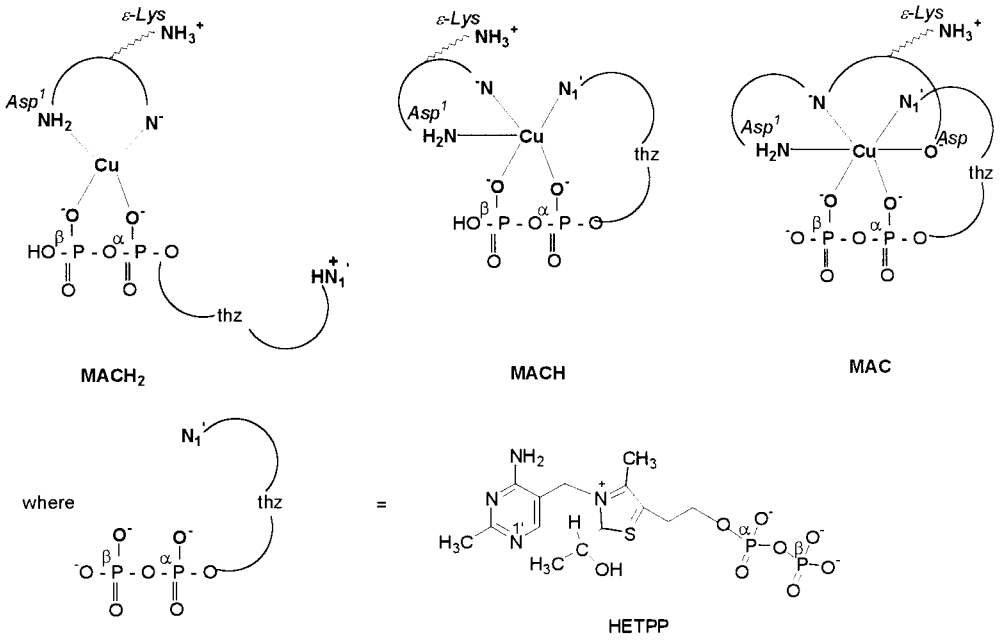


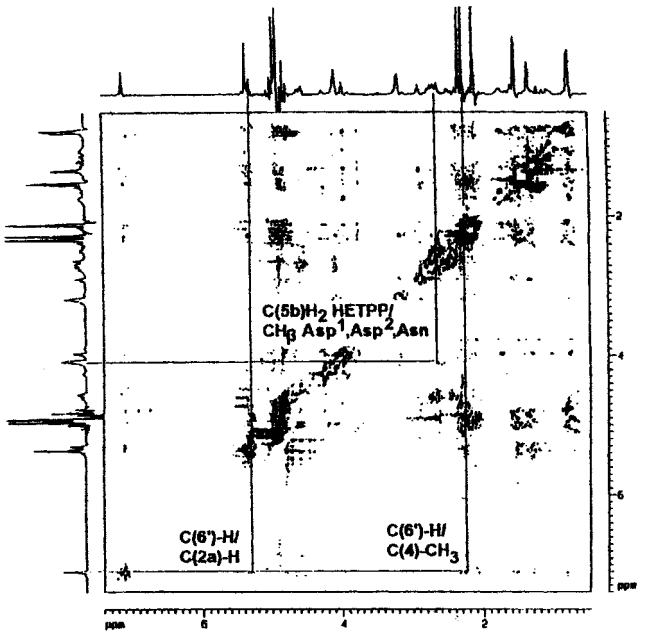


**Figure 7.** $^1H-^1H$ ROESY spectrum of the tertiary $Cu^{2+}$−peptide−HETPP system at pH 7.2.

The temperature was chosen in order to take advantage of the relative sharpening of the signals which are broadened by the magnetic interaction with the paramagnetic copper. Although the presence of a paramagnetic center leads to a weakening or disappearance of the NOE phenomenon,[21] in our case, the ROESY spectrum shows a large number of cross peaks due to the low concentration of $Cu^{2+}$ in the $Cu^{2+}$−peptide−HETPP system (ratio of $Cu^{2+}$/peptide/HETPP = $(3.9 \times 10^{-2})$:2:4 mM, at pH 7.2, as in the one-dimensional spectrum). Because both HETPP and peptide constitute the coordination sphere of copper, this imposes a close proximity between them and results in the following cross peaks: C(5b)$H_2$ from HETPP with $\beta$-CH of $Asp^1$, $Asp^2$, or Asn as well as C(2′)-$CH_3$ from HETPP with α-CH of $Asp^1$, $Asp^2$, or Asn. These observations support once more the proposed coordination environment of Cu(II) in the tertiary $Cu^{2+}$−peptide−HETPP system.

The important intramolecular cross peaks observed are those between the protons C(6′)−H/C(2a)−H and C(6′)−H/C(4)−$CH_3$ from the HETPP molecule. The former clearly indicates that the pyrimidine C(6′)−H proton is directed to the thiazole ring. This spectroscopic feature is characteristic of the thiamin derivatives that adopt the S conformation.[4] The latter cross peak between the C(6′)−H and the C(4)−$CH_3$ suggests that the thiazole ring was rotated in the same manner as in the crystal structure of HETPP.[7c] On the basis of these observations, we conclude that the S conformation, which was found in the crystal structure of the HETPP and in aqueous solutions of metal−HETPP complexes, is retained also by HETPP in the aqueous solutions of the tertiary $Cu^{2+}$−peptide−HETPP system.

## Conclusion

In summary, in the present study, the coordination ability, as a function of pH, of both HETPP and peptide Asp-Asp-Asn-Lys-Ile toward copper(II) has been demonstrated. The existence of a tertiary $Cu^{2+}$−pentapeptide−HETPP complex around physiological pH is presented, and it has a particular biological interest. In this system, the peptide which mimics the protein environment of the metal binding site Asp185-Asp186-Asn187-Lys188-Ile189 of transketolase offers three coordination sites

(21) Paudler, W. W. *Nuclear Magnetic Resonance*; Wiley-Interscience Publications: New York, 1987.

to the metal ion, the terminal amino group, the side chain of one Asp, and one main chain nitrogen. The coordination sphere is completed by two phosphate oxygens of the coenzyme as in the crystal structures of the enzymes,[3] and instead of a water molecule, the N(1′) of the pyrimidine ring is bound. The adopted conformation of the thiamin molecule is the S one. These findings bear relevance to the enzymic action of thiamin in vivo.

Thus, the present data show that *in solution* the observed conformation of the coenzyme around physiological pH is not the V but the S. The S conformation together with the F represents lower energy states than the "active V"[1d] found in the crystal structures of TPP-dependent enzymes.[3] On the other hand, Crout et al.[9b] have suggested that energy minimization of intermediate HETPP brings the deprotonated 4′-imino group into close contact with the 2-α-hydroxyl group, forming a strong hydrogen bond with the hydroxyl proton. In this model, such a close contact of the 4′-imino group to the hydroxyl group assumes that the HETPP adopts the V conformation. However, it has been mentioned earlier that HETPP−metal complexes which present a direct N(1′)−metal bond and hold the S conformation are able to release acetaldehyde during enzymic studies.[6] This indicates that a metal−N(1′) bond and the S conformation in this catalytic step do not occlude the catalytic cycle. Furthermore, it is suggested that while the V conformation of thiamin is active possibly in one of the initial steps of catalysis, the S conformation should also be of importance in the catalytic cycle. These findings substantiate our previous proposal[7a] that if N(1′) is used as a metal coordination site *during* the catalytic cycle, then the coordination to N(1′) should happen *after* the formation of the "active aldehyde" intermediates which will adopt the S conformation.

**Supporting Information Available:** Assignment of $^{1}$H NMR spectra of the free peptide (Table S1) and of the $Cu^{2+}$−peptide−HETPP system (Table S2), assignment of $^{13}$C NMR spectrum of the free peptide (Table S3), and two-dimensional $^{1}$H−$^{1}$H TOCSY, $^{1}$H−$^{13}$C HMQC, and $^{1}$H−$^{13}$C HMBC spectra (Figures S1, S2, and S3). This material is available free of charge via the Internet at http://pubs.acs.org.

IC001465T